(NASA-CR-174248) THE EVALUATION OF A DEFORMABLE DIFFRACTION GRATING FOR A STIGMATIC EUV SPECTROHELIOMETER Progress Report, 15 Aug. - 30 Nov. 1984 (Stanford Univ.) 10 p HC A02/MF A01 CSCL 20F G3/74

N85-16611

Unclas 13039

C S S A

CENTER FOR SPACE SCIENCE AND ASTROPHYSICS

STANFORD UNIVERSITY

Stanford, California

THE EVALUATION OF A DEFORMABLE DIFFRACTION GRATING

FOR A STIGMATIC EUV SPECTROHELIOMETER

Progress Report for NASA Grant NAGW-540
for the period 15 August to 30 November 1984

J. Gethyn Timothy
Principal Investigator

Center for Space Science and Astrophysics
Stanford University
Stanford, California 94305

An interim progress report is being submitted at this point in time in order to bring the reporting period into phase with the grant renewal period.

During the past four months, a second toroidal replica grating was fabricated by Hyperfine, Inc., using the set-up procedures described in the last progress report, and as discussed in the attached report by M. C. E. Huber, was found to have an aspect ratio within 10% of the desired value. It still appears that the aspect ratio of the replica toroidal gratings is tending to come out somewhat low, and one of the objectives of the next few months will be to determine whether this is caused by some relaxation in the epoxy or some residual error in the setup when the replication is made from the deformable submaster grating.

During the past few weeks, the first imaging tests at EUV wavelengths near 500 Å have been carried out by G. Tondello in the laboratory at Padua. The initial results are most encouraging with blur sizes of the order of, or less than, 40 microns. Further focussing and additional photographic tests will be carried out between now and the end of the year, and preparations will be made for the first photoelectric measurements of the image quality using the (256 x 1024)-pixel MAMA detector system during the first half of 1985.

To this end, the visible-light (256 x 1024)-pixel MAMA detector tube has now completed initial evaluation in the laboratory at Stanford and is ready to be used on this program. Similarly, the (256 x 1024)-pixel, open-structure EUV detector tube is also ready for evaluation in the laboratory at Stanford.

ATTACHMENT

Report on Hyperfine Grating #616-2-3

by

M. C. E. Huber

Report on test of second 3600-l/mm toroid grating (Hyperfine No. 616-2-3, 1 m average radius of curvature, ruled surface 70 mm × 70 mm, Os coated)

Summary

MCEH has measured the aspect ratio of Hyperfine grating No. 616-2-3 in a laser Twyman–Green interferometer and found a value $R_v/R_h = 0.9809$. This compares with the specified value $(R_v/R_h)' = 0.9782$. The deviation from a sphere results in ± 18.5 fringes at $\lambda = 632.8$ nm (as compared to ± 21.4 fringes for the specified aspect ratio and ± 10.5 fringes on the previous replica). The resulting wavelength range with a maximum blur of 25 μm is 60.9 to 46.2 nm, implying angles of incidence $\alpha = 11°.11$ and diffraction $-\beta_0 < \beta < \beta_0$ with $\beta_0 = 1°.52$. The aspect ratio of the grating is acceptable.

1. Introduction

This is a report on the toroidal Hyperfine replica grating No. 616-2-3. This grating replaces the previous replica, which was found to have too mild a toroid.

Following the determination of the aspect ratio, which was performed at ETH Zürich on August 29, 1984 and is described below, the grating 616-2-3 will undergo tests with ultraviolet radiation in the 1-m vacuum spectrograph at CNR's Centro di Studio sui Gas Ionizzati in Padova.

2. Check on stigmatic focus in zero order

As pointed out in § 4 of the report on the preliminary test of the previous replica, a toroid of the specified aspect ratio $(R_v/R_h)' = 0.9782$ (where R_v and R_h are the radii of curvature in the vertical and horizontal planes, i.e. along and across the grating rulings, respectively)

would show a stigmatic image with an angle of incidence and reflection of $\gamma' = 8^\circ.4907$, or with a lateral distance of ca. 300 mm between source and image (cf. Fig. 3). A quick check of grating No. 616-2-3 showed that this was nearly the case. Since this test is considerably less sensitive than the interferometric test, the exact lateral distance was not determined directly.

With the benefit of hindsight — namely after the interferometric test — we calculate that the actual lateral distance would have been given by

$$R_v/R_h = 0.9809 = \cos^2\gamma \tag{2.1}$$

or $\gamma = 7^\circ.9466$ and thus

$$b = 2R_h \sin\gamma = 2 \times 1009.7\text{mm} \times \sin\gamma = 279.2\text{mm}. \tag{2.2}$$

The test of the stigmatic focus thus provides a confirming check of the wavefront measurements.

3. Determining the wavefront in a Twyman–Green interferometer.

By use of the setup shown in Fig. 1, we compared the wavefront reflected by the toroidal grating with a spherical wavefront. The fringes trace contour lines, i.e. lines of equal height above or below a spherical surface. Going from one fringe to the next corresponds increasing (or decreasing) the height by $\lambda/2$ (with $\lambda = 0.6328\,\mu$m). A photograph of the fringe pattern is shown in Fig. 5.

The measured height differences going from the center to the edges on the top (or bottom) and on the sides of the 70×70 mm^2 aperture — was ca. ± 18.5 fringes. This corresponds to a height difference of

$$\begin{aligned} \pm\delta &= \pm(\text{fringes} \times \lambda/2) = \pm(18.5 \times 0.6328/2) \\ &= \pm 5.85\,\mu\text{m} \end{aligned} \tag{3.1}$$

or to a total height difference at the centers of the edges of

$$\Delta = h_v - h_h = 2\delta = 11.71\,\mu\text{m}. \tag{3.2}$$

We u e the geometrical relations defined by Fig. 2 and obtain:

$$\Delta = h_v - h_h = \frac{a^2}{2}\left(\frac{1}{R_v} - \frac{1}{R_h}\right) = \frac{a^2}{2R^2}(R_h - R_v) = \frac{a^2}{2R}\left(1 - \frac{R_v}{R_h}\right) \tag{3.3}$$

where R is the (average) radius of the flexible grating in its spherical state. (It was assumed throughout that $h \ll R$, so that terms of the order of h^2 could be neglected, and that $R_v \cdot R_h = R^2$.)

From the interferometric measurement we thus obtain the aspect ratio, which is given by equ. (3.3), but is derived differently as a check on the approximations used:

$$\begin{aligned} \frac{R_v}{R_h} &= \frac{R - \frac{R_h - R_v}{2}}{R + \frac{R_h - R_v}{2}} = \frac{R - \frac{R^2\Delta}{a^2}}{R + \frac{R^2\Delta}{a^2}} \simeq 1 - \frac{2R\Delta}{a^2} \\ &= 1 - \frac{2 \times 10^3\text{mm} \times 11.71 \times 10^{-3}\text{mm}}{35^2\text{mm}^2} = 0.9809 \end{aligned} \tag{3.4}$$

4. Stigmatic wavelengths of present grating

The condition for stigmatic imaging with a totoidal grating is

$$R_v / R_h = \cos\alpha \cos\beta_0 \tag{4.1}$$

where α and β_0 are the angles of incidence and diffraction, respectively, that apply for a stigmatic focus.

The wavelengths for stigmatic conditions that are available with the present grating can be calculated from equ. (4.1) and the grating equation

$$n\lambda = d(\sin\alpha + \sin\beta_0) \tag{4.2}$$

where the order is assumed to be $n = 1$ and the grating constant is $d = 2777.8\,\text{Å}$.

If the blur at the central wavelength $\lambda(\beta = 0°)$ should not exceed 25 μm (i.e. one pixel of the present MAMA detector) we must chose $|\beta_0| \leq 1°.53$. The wavelengths at the upper limit of $|\beta_0|$ are therefore

$$\begin{aligned} \lambda(\beta_0 &= -1°.53) = 461\,\text{Å} \\ \lambda(\beta &= +0°.00) = 536\,\text{Å} \\ \lambda(\beta_0 &= +1°.53) = 610\,\text{Å} \end{aligned} \tag{4.3}$$

For $\beta_0 = 0$ we obtain

$$\lambda(\beta_0 = +0°.00) = 540\,\text{Å}, \tag{4.4}$$

The respective angles of incidence α are 11°.1164 and 11°.2201.

The stigmatic wavelength ranges for given maximum blurs are plotted in Fig. 4. The plot is based on a focal surface that is either flat and coinciding with the vertical focus, or curved and coinciding with the Rowland circle (of diameter R_h). The maximum blur can be reduced, if a "hybrid" focal surface is chosen, which lies in between (and equidistant from) the vertical and horizontal foci. In this case, the observed maximum blur would be nearly half that occuring on the "pure" focal surfaces, so that the wavelength range is somewhat wider than that shown in Fig. 4. On the other hand it should be realized that Fig. 4 is valid for in-plane images only, and that larger blurs apply, if the light source lies out of plane.

5. Conclusion

The present aspect ratio permits a test of the grating in the 1-m vacuum-ultraviolet spectrograph in Padova. Given an acceptable maximum blur of 25 μm, the stigmatic wavelength range accessible with the grating extends from ca. 44 to 63 nm.

It will be interesting to see, what is responsible for the difference between the specified and the actual aspect ratio. Can the difference be explained by the shrinking of the epoxy layer supporting the replica?

Zurich, September 6, 1984

Martin C.E. Huber

Fig. 1 Twyman-Green Interferometer

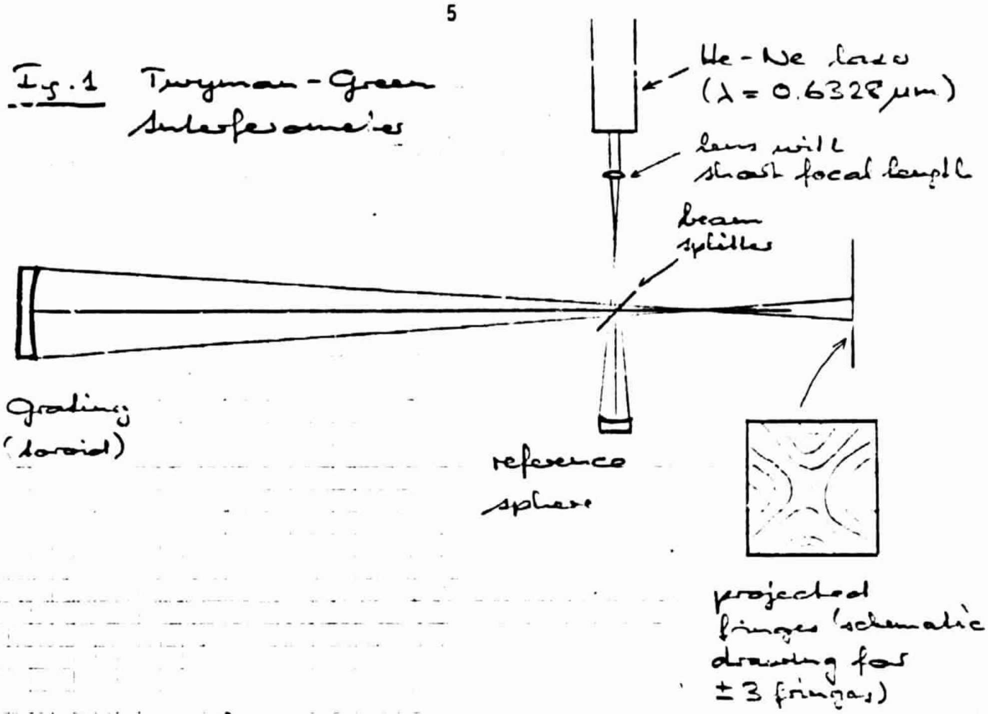

Fig. 2 Calculating h

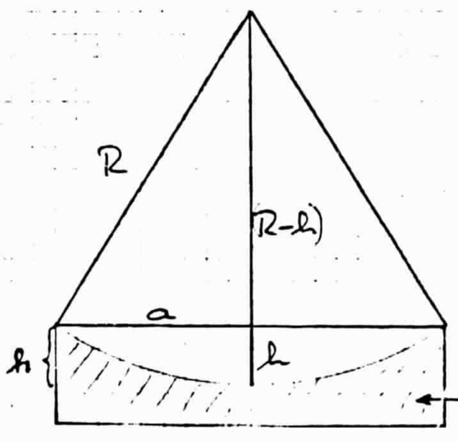

(enlarged grating substrate)

$$(R-h)^2 = R^2 - a^2$$

$$-2Rh = -a^2$$

$$h = \frac{a^2}{2R}$$

Fig. 3 Stigmatic focus in zero order.

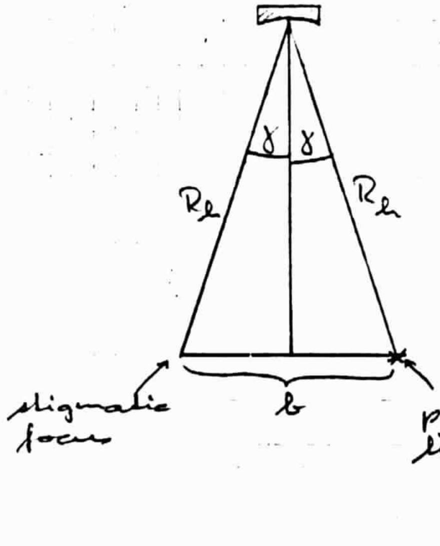

$$\frac{R_v}{R_h} = \cos\gamma \cdot \cos(-\gamma) = \cos^2\gamma$$

$$b = 2R_h \sin\gamma$$

Fig. 5 Photograph of fringe pattern in laser Twyman-Green interferometer.

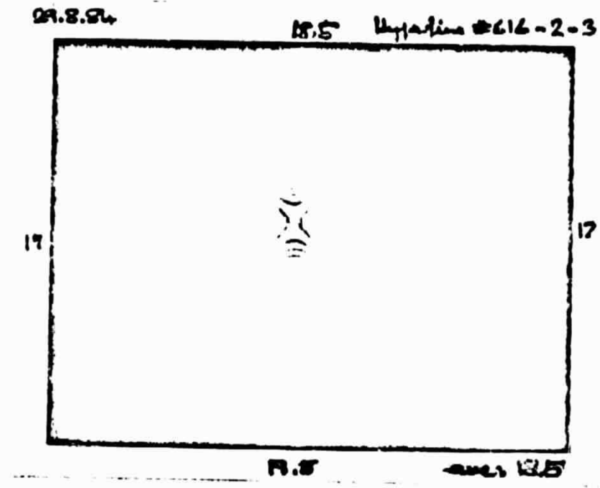

Fig. 4 Stigmatic wavelength ranges for given blur on horizontal-focus or vertical-focus surfaces.